Program Digest, 2019 IEEE International Ultrasonics Symposium (IUS)
Glasgow, Scotland, October 6-9, 2019

Development of a 1-D Linear Phased Ultrasonic Array for Intravascular Sonoporation

Alexandru C. Moldovan, Zhen Qiu, David Lines, Anthony Gachagan
Centre for Ultrasonic Engineering
University of Strathclyde
Glasgow, United Kingdom
alexandru.moldovan@strath.ac.uk

Sandy Cochran
Medical and Industrial Ultrasonics
University of Glasgow
Glasgow, United Kingdom

***Abstract*—Therapeutic efficiency of sonoporation is hampered by ultrasound attenuation, low focusing efficiency due to beam scattering from the variety of tissues in the propagation path, and heating. This paper describes the manufacturing and characterization of miniature 1-3 connectivity 1-D linear phased arrays of the size of an 8 Fr catheter for intracorporeal sonoporation. Their advantage over external transducers is that ultrasound is delivered closer to the target tissue which reduces aberration in the propagation path. Four arrays with resonant frequencies of 1.5 MHz and 3.0 MHz were manufactured using the traditional dice and fill method. The piezoelectric materials were ceramic (PZT-5H) and single crystal (PMN-29%PT). The piezocomposite design was optimised for lowest peak negative pressure (PNP) through a simulation approach using PZFlex (Onscale, CA, US). A comparison between the simulated electrical impedance of individual array elements and the experimental data shows the coupling coefficient (k_t) is reduced in the real transducers, but the electrical resonance frequency and modes are well predicted by the simulation. The lower k_t and the lack of electrical interconnects in the simulation led to lower measured PNP values than the simulation. However, the normalized beam shapes strongly agree between the two cases.**

Keywords—medical ultrasound; intravascular; sonoporation; targeted drug delivery; 1-D ultrasonic linear phased array.

I. CLINICAL BACKGROUND AND MOTIVATION

The combination of ultrasound and gas-filled contrast agents represents a promising approach for enhancing drug and gene delivery on a cellular level [1], [2]. Most often, therapeutic agents affect not only the diseased tissue but also the surrounding healthy tissue [1]. The toxicity of the drug limits the allowed dosage and thus its potential therapeutic effect. Cancer treatment is one example in which inefficient drug delivery to the tumor leads to a wide range of side effects [1]. Sonoporation represents a non-invasive targeted drug delivery method that aims to increase drug concentration in the tumor while sparing the healthy tissue by use of focused ultrasound. The main mechanism of sonoporation is considered to be the cavitation of gas-filled contrast agents (GCA) near cells [3]. This creates short lived pores in the plasma membrane which, in turn, increases cellular permeability to exogenous agents [2].

Some of the current difficulties with therapeutic ultrasound delivered by external transducers include obstacles in the ultrasound propagation path, transducer and tissue heating, low focusing power, reduced penetration depth and tissue motion due to breathing [4]. One way to minimize these difficulties is to reduce the ultrasound path between the transducer and the target tissue by performing intracorporeal therapy.

II. AIM OF STUDY

The work outlined here is focused on manufacturing and characterization of miniature 1-3 connectivity 1-D linear phased arrays that can be fitted inside an 8 Fr catheter with the purpose of delivering ultrasound from within a larger blood vessel. The advantage of using phased arrays for sonoporation consists in their ability to electronically steer the ultrasound beam at different angles and depths in tissue, thus reducing the mechanical movement of the catheter inside the patient's body as well as increasing the procedure's accuracy. A major limitation in the design of catheter arrays is the thickness of the active element which varies in inverse proportion with the frequency of resonance. This aspect is particularly important as cell permeabilisation decreases with insonation frequency [1]. Also, attenuation and heat deposition in the tissue increase with frequency [5]. Higher frequencies also have less effect on microbubbles as commercial gas-filled contrast agents usually have resonance frequencies between 1 and 3 MHz [6, 7]. The required reduced transducer length limits the number of array elements which, in turn, leads to poor focusing capability, while the reduced elevation increases ultrasound beam spreading with range.

Through a finite element analysis (FEA) approach, we have previously demonstrated that a catheter phased array can achieve peak negative pressure (PNP) values that are well within sonoporation thresholds [8]. The composite parameter sets for the transducers manufactured for this study were determined using a similar software optimization approach as detailed in [8]. A cross comparison between the manufactured arrays and the simulation is reported here in order to demonstrate the reliability of the software model.

III. TECHNICAL BACKGROUND

Four composite arrays were manufactured using the well-established dice-and-fill method. The design parameters (Table I) were chosen to be as close as possible to the set provided by FEA optimization, but, importantly, to comply with the manufacturing capabilities of the dicing system with regard to blade thickness, protrusion and spatial accuracy.

Mr. Moldovan's PhD Studentship is funded through an Engineering and Physical Sciences Research Council (EPSRC) Doctoral Training Grant (EP/N509760/1)

TABLE I. COMPOSITE TRANSDUCER PARAMETERS

Active Material	FE (MHz)	VF (%)	AR (%)	Kerf (μm)	Thk (μm)	Width (mm)	Length (mm)
PZT-5H	1.5	70	42.0	80	983	2.36	11.65
	3.0	70	42.0	41	489	2.46	7.95
PMN-29%PT	1.5	72	58.1	74	724	2.37	11.68
	3.0	78	59.3	29	372	2.47	7.97

Epofix (Struers, UK) was used to fill the composite kerfs of all transducers. The 1.5 MHz arrays had 24 elements and the 3.0 MHz were limited to 32 elements to match the maximum channel count of the phased array controller. In all transducers, the element pitch was less than or equal to half wavelength to avoid grating lobe effects.

Transducer electroding was performed with a two-part solvent-resistant electrically conductive Ag ink (Creative Materials Inc., Ayer, MA) due to its superior mechanical properties and electrical resistance compared with conventional fast drying alcohol-based Ag paint. Backing was added only to provide support for the transducer's active element and to fill any empty space in the casing. The backing material was a mixture of air-filled microballoons and Epofix, to achieve a large impedance mismatch with the active element to maximize forward energy transmission into the tissue. The electrical interconnects to the array elements were done with a flexi-circuit bonded using anisotropic conductive adhesive (Creative Materials Inc., Ayer, MA).

Electronic beam steering of the array was performed with a 32-element FIToolbox™ phased array controller coupled to the flexi-circuit with 0.5 m long micro-coaxial cables.

IV. METHODOLOGY

A. Transducer Electroding

Three methods of applying Ag ink coatings were investigated for the transducer electrodes. The procedure was tested on glass microscope slides to facilitate a high number of test samples. Brush coating produced uneven layers with thicknesses varying from 1.0 μm to 20 μm which affected the electrical resistance of the electrode due to non-uniform curing. K bar coaters with 18 μm and 6 μm wire diameters produced thin and uneven layers with high electric resistance (>15 Ω). The quality of the Ag ink layer also varied significantly between different samples for both aforementioned methods due to the nature of the coating process. Spin coating however produced reproducible uniform layer thicknesses with low electrical resistance and was the preferred method.

The layer quality depended on the rotation speed, spin time, ink and thinner quantity. A solvent thinner was added to the two-part conductive ink mix to improve its spread during spin coating. Any air bubbles trapped in the ink mixture were removed after exposure to 4 cycles of vacuum degassing for a total of 10 min. Curing temperature and time were also determining factors for the electrode quality. The films on the PZT-5H samples were cured at 75°C for 4 hr and those on the PMN-PT samples at 50°C for 80 hr. 75°C was selected as a maximum to avoid softening of the Epofix kerf filler and 50°C was selected to avoid the piezocrystal from depoling. Long curing times were required because the selected curing temperatures were below the minimum 80°C requirement set by the manufacturer. The downside of using lower curing temperatures is reduced layer resistance to solvents like acetone or isopropanol. Table II shows a summary of the test cases and results.

TABLE II. SUMMARY OF ELECTRODE TEST CASES

RPM	Curing Temp (°C)	Curing time (hr)	Resistance (Ω)	Thickness (μm)
2000	75	4	0.7	9.6
2500	75	4	1.0	6.2
3000	75	4	1.3	4.8
	50	80	1.4	4.7
3500	75	4	1.9	4.1
	50	80	1.3	4.0
4000	75	4	2.0	4.2
5000	75	4	3.7	2.5
6000	75	4	5.9	2.2

The finished electrode applied to the PZT-5H transducers demonstrated satisfactory mechanical resistance to detachment by dicing machine tape, whereas the electrode applied on the PMN-PT samples presented missing regions. This can be attributed to the low curing temperature used for the single-crystal transducers. Because the electrode thickness was greater in the case of 2000 rpm than 3000 rpm and the resistance of the layer was similar, a decision was made to use 3000 rpm to coat the transducers. The electrical resistance of the electrodes applied to the PZT-5H transducers was 0.5 Ω, and for PMN-PT was 0.6 Ω, about half the value measured on the glass slides.

The spin time did not have such a significant effect on the electrode quality as the rotation speed. However, it was observed that for lower rotation speeds, higher spin time achieved enhanced consistency mostly in terms of reducing layer thickness, with less effect on electrical resistance. In terms of higher rotation speeds, shorter spin times led to lower electrical resistance of the layer. Spin coating time for all transducers was set to 15 seconds. In order to protect the deposited front electrodes and ensure waterproofing, the arrays were covered with a thin layer of insulating varnish.

B. Transducer Characterization

Electrical impedance spectroscopy was performed on the transducers with an Agilent 4395A impedance analyser after the flexi-circuits were bonded. No measurements were performed on the bare arrays at earlier stages in the manufacturing process to avoid damaging the fragile transducer elements. The acoustic field of the manufactured arrays was measured with a needle hydrophone (NH) (Precision Acoustics Ltd, Dorchester, United Kingdom) with a diameter of 0.2 mm, scanned by a 3-axis flatbed configuration linear stage with an increment size of 0.2 mm. The scan step size and NH diameter were chosen to comply with the British Standard for Ultrasonics – Hydrophones (BS EN 62127-1:2007+A1:2013) for both sonication frequencies.

The FEA models consisted of two different frameworks, one for simulating the electric impedance of the transducer, and the other for acoustic pressure mapping with water loading. Both types of FEA models were evaluated in 3D using PZFlex

(Onscale, CA, USA). For the impedance model, one element in the array was excited with a half-cycle sine wave, while all other elements were left open circuit. The simulation time was calculated to allow the transducer to ring down in order to obtain reliable impedance plots. Backing material was included in the impedance simulations only for the 1.5 MHz arrays and not for the 3.0 MHz ones because of computational limitations. Quarter symmetry was also applied to reduce the computational demands.

The acoustic pressure model included the full backing layer for the 1.5 MHz arrays and a reduced size backing for the 3.0 MHz devices, again, due to computational demands. The electrical signal applied to the transducer comprised a 10-cycle burst and the simulation time was set to allow all ultrasound pulses from all array elements to pass through and exit the water load in the model. The simulation time for the pressure model was on average a quarter of the simulation time for the impedance models, allowing more features to be added to the model with similar computation requirements. The model had no symmetry and contained a minimal water load coupled to the transducer. The time-varying acoustic pressure in a much larger water load was simulated using time response extrapolations at equally spaced points in a 2D plane fixed at the center of the array and stretching in the XZ directions (array length – water depth). PNP was extracted from the time-amplitude data by determining the minimum of each pressure trace. In order to maintain consistency with the manufactured transducers, both the backing layer material and the Epofix kerf filler were acoustically characterized before being included in the FEA models.

V. Results and Discussion

Both the 1.5 MHz and the 3.0 MHz transducers were focused at 5.0 mm in the axial direction at 0°, 15°, 30° and 40°. The same steering delays and driving voltages for each beam steering case were used in both the FEA model and for the FIToolbox™ to maintain consistency. Fig. 1 provides a comparison between the simulated (sim) and experimental (exp) PNP maps for the 1.5 MHz PMN-PT array steered at 0° and 40° at 5.0 mm distance.

As Fig. 1 shows, the simulation predicts the beam shape accurately for both steering angles. Similar results were obtained at 15° and 30°. The decrease in PNP between the predicted and measured results can be attributed to factors ranging from electrical impedance mismatch between the phased array controller and the array elements, interelement crosstalk, non-ideal drive signals from the FIToolbox™, and the reduced transducer k_t, Fig. 2. The simulation also excluded the effect of the anisotropic conductive adhesive on clamping the transducer or the resultant electrical cross coupling. The flexi-circuit was also not considered in the simulation because its structure was difficult to mesh.

Pressure profiling was repeated for the 3.0 MHz PMN-PT array and is presented in Fig. 3, the only difference being the array was driven at a lower voltage than the lowest the FIToolbox™ power supply can deliver with the purpose to protect the NH from excess mechanical index (MI). This was achieved by reducing the signal duty cycle to 10%.

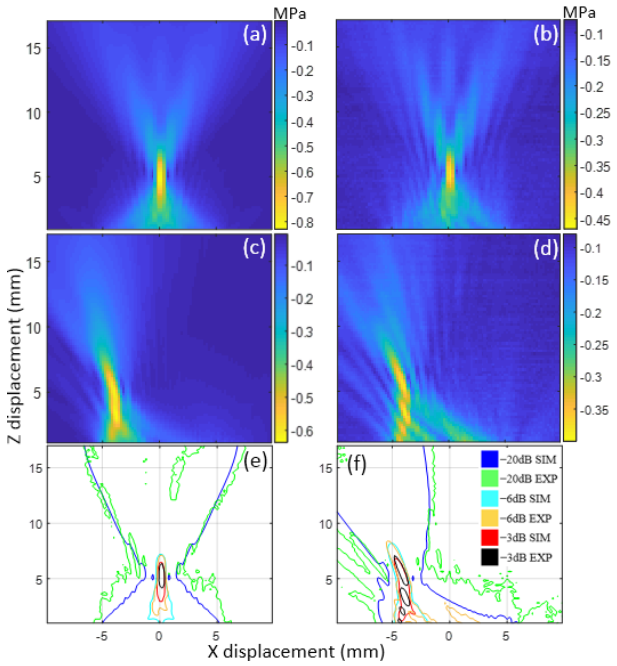

Fig. 1. 1.5 MHz, PMN-PT array with focal point at 5 mm: (a), (c) simulation PNP profiles at 0° and 40°; (b), (d) measured PNP profiles at 0° and 40°; (e), (f) superimposed dB contours of simulated and experimental data.

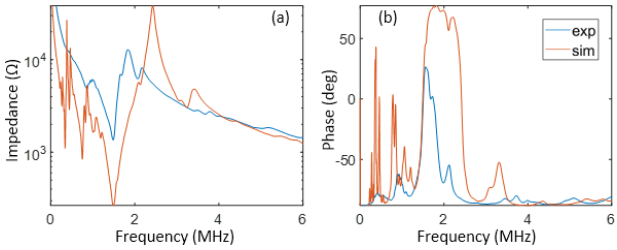

Fig. 2. 1.5 MHz, PMN-PT element 12: (a) electrical impedance; (b) phase.

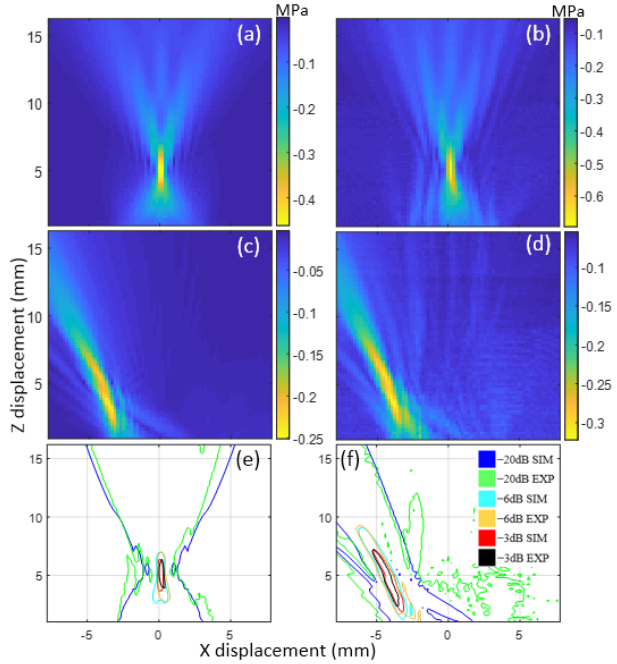

Fig. 3. 3.0 MHz, PMN-PT array with focal point at 5 mm: (a), (c) simulation PNP profiles at 0°and 40°; (b), (d) measured PNP profiles at 0°and 40°; (e), (f) superimposed dB contours of simulated and experimental data.

The impedance and phase plots in Fig. 4 show that the manufactured transducer has a distinct mode intermediate between the series and parallel resonances compared to the simulated one. This mode is probably increased by the flexi-bonding which added clamping to the electrodes.

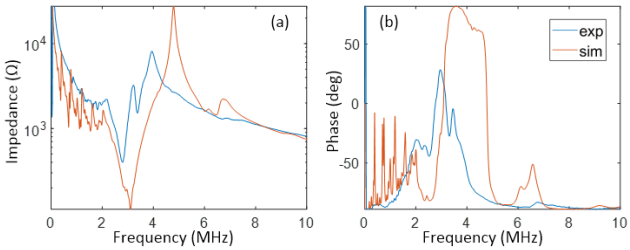

Fig. 4. 3.0 MHz, PMN-PT element 18: (a) electrical impedance; (b) phase.

In order to demonstrate the capability of the arrays to achieve MI values in the range required for sonoporation, a sweep of the driving voltage was performed and related to the MI measured at the focal point, Fig. 5. The output of the 3.0 MHz PMN-PT array is not included in the graph because the excitation signal from the FIToolbox™ was altered to protect the NH and V_{p-p} was no longer relevant.

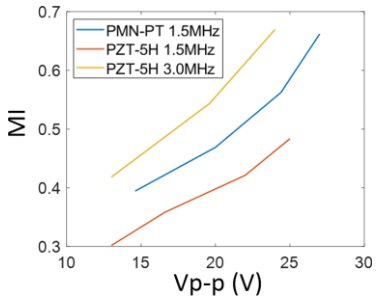

Fig. 5. Measured MI as function of peak-to-peak excitation voltage (V) for fabricated arrays.

The low driving voltages required for the arrays are an advantage for safe use inside the vasculature and are well within the limits supported by the flexi-circuits and microcoaxial cables. Despite PMN-PT being non-ideal for high power applications, Fig. 5 shows that the 1.5 MHz binary piezocrystal array achieves significantly higher MI than its PZT-5H counterpart. Moreover, the reduced thickness of the single crystal compared to the ceramic is important for catheter implementation because space is limited.

VI. SUMMARY AND CONCLUSIONS

With the aim to develop 8 Fr transducer arrays able to induce sonoporation, a software model based on FEA and extrapolation was compared with experimental transducers and provided good correlation in terms of acoustic pressure profiles. This required the development of a method to apply permanent electrodes to the transducer using a two-part electrically conductive, heat-curing Ag ink as a replacement for the temporary fast-curing Ag paint and the difficult and expensive procedure of metal deposition through evaporation.

Two different types of piezoelectric materials and two different resonant frequencies were included in the study and the results proved similar. The PNP values predicted by the software model are in all cases approximately double that in the experimental case. This can be attributed to lower coupling coefficients of the manufactured transducers, electrical impedance mismatch between the FIToolbox™ controller and the transducer elements, connecting wires and transducer features that were not simulated, including anisotropic conductive adhesive, flexi-circuit, and non-ideal drive signal.

This study showed that FEA can be used to successfully predict the beam shape of a miniature 1-D linear phased array at different steering angles in a water load. This can provide particularly useful insight into array focusing in tissues, where a NH cannot be readily moved in order to perform acoustic mapping. Therefore, this FEA approach could be used for therapy planning for intravascular sonoporation. Given the good correlation between the FEA simulation and the manufactured transducers' pressure profiles, data provided from a NH inserted at a known point in the tissue can be used as reference for the pressure amplitude distribution in the target.

The MI levels obtained with the manufactured transducers successfully match those required for sonoporation and potentially even for high intensity focused ultrasound, demonstrating their validity for therapeutic ultrasound. The operating voltages are low, which is helpful for catheter realization.

Further work will focus on testing the sonoporation efficiency of the arrays in an *in-vitro* model, followed by a cadaver model and an *in-vivo* trial.

ACKNOWLEDGMENT

We are grateful for the PZFlex research license provided by OnScale, CA, USA.

REFERENCES

[1] R. Karshafian, P. D. Bevan, R. Williams, S. Samac, and P. N. Burns, "Sonoporation by Ultrasound-Activated Microbubble Contrast Agents: Effect of Acoustic Exposure Parameters on Cell Membrane Permeability and Cell Viability," Ultrasound in Medicine & Biology, vol. 35, no. 5, pp. 847–860, May 2009.

[2] S. Mehier-Humbert, T. Bettinger, F. Yan, and R. H. Guy, "Plasma membrane poration induced by ultrasound exposure: Implication for drug delivery," Journal of Controlled Release, vol. 104, no. 1, pp. 213–222, May 2005.

[3] H.-D. Liang, J. Tang, and M. Halliwell, "Sonoporation, drug delivery, and gene therapy," Proc Inst Mech Eng H, vol. 224, no. 2, pp. 343–361, Feb. 2010.

[4] S. Bobkova, L. Gavrilov, V. Khokhlova, A. Shaw, and J. Hand, "Focusing of high-intensity ultrasound through the rib cage using a therapeutic random phased array," Ultrasound Med Biol, vol. 36, no. 6, pp. 888–906, Jun. 2010.

[5] A. Y. Cheung and A. Neyzari, "Deep Local Hyperthermia for Cancer Therapy: External Electromagnetic and Ultrasound Techniques," Cancer Res, vol. 44, no. 10 Supplement, pp. 4736s–4744s, Oct. 1984.

[6] S. M. van der Meer, M. Versluis, D. Lohse, C. T. Chin, A. Bouakaz, and N. de Jong, "The resonance frequency of SonoVue/spl trade/ as observed by high-speed optical imaging," in IEEE Ultrasonics Symposium, 2004, 2004, vol. 1, pp. 343-345 Vol.1.

[7] C. Lazarus, A. N. Pouliopoulos, M. Tinguely, V. Garbin, and J. J. Choi, "Clustering dynamics of microbubbles exposed to low-pressure 1-MHz ultrasound," The Journal of the Acoustical Society of America, vol. 142, no. 5, pp. 3135–3146, Nov. 2017.

[8] A. C. Moldovan, J. Dziewierz, A. Gachagan, S. Cochran, and H. S. Lay, "Virtual Prototyping of a Catheter Transducer Array for Internal Hepatic Sonoporation," 2018 IEEE International Ultrasonics Symposium (IUS), pp. 1–4, 2018.